Aniline Polymerization into Montmorillonite Clay: A Spectroscopic Investigation of the Intercalated Conducting Polymer

Gustavo M. do Nascimento,[†] Vera R. L. Constantino,[†] Richard Landers,[‡] and Marcia L. A. Temperini*,[†]

Departamento de Química Fundamental, Instituto de Química, Universidade de São Paulo, CP 26.077, CEP 05513-970, São Paulo, SP, Brazil, and Departamento de Física Aplicada, Instituto de Física Gleb Wataghin, Universidade Estadual de Campinas, CP 6165, CEP 13083-970 Campinas, SP, Brazil, and Laboratório Nacional de Luz Sincrotron, CP 6192 13084-971, Campinas, SP, Brazil

Received May 13, 2004; Revised Manuscript Received September 9, 2004

ABSTRACT: The polymerization of aniline intercalated into montmorillonite clay was monitored by in situ UV−vis−NIR and resonance Raman spectroscopies and in situ small-angle X-ray scattering. In the initial stages of the polymerization, it is observed the PANI−ES polaronic band at 750 nm in the UV−vis−NIR spectrum and also the characteristic PANI-ES resonance Raman spectrum (excited at 632.8 nm), which indicate that the head-to-tail coupling reactions between anilinium radical cations are occurring. Nevertheless, the resonance Raman spectrum excited at 488.0 nm presents bands at 1211, 1370, 1455, and 1608 cm^{-1}, assigned to the benzidine dication species, which suggests that tail-to-tail coupling reactions are also occurring. In the final stages of polymerization, the presence of electronic absorption bands at 670 and 620 nm indicates the formation of new chromophoric species, which is also confirmed by its peculiar resonance Raman spectrum at 632.8 nm wavelength. The in situ SAXS results show that, during the anilinium polymerization in aqueous clay suspension, the interlayer spacing is ca. 19 Å. XRD diffraction pattern and SEM images of the powder PANI−MMT nanocomposites indicate that the polymerization occurs mainly between the clay layers, and the basal spacing is ca. 13.2 Å. While the IR spectra of nanocomposites show only bands due to PANI−ES-like segments, resonance Raman and nitrogen XANES techniques lead to the presence of PANI−ES-like chains, benzidine segments, azo bonds, and phenazine-like rings in the structure of the confined conducting polymers. The XPS technique detects only PANI−ES segments of the polymeric structure, suggesting that on the external surface and/or on the edge of clay crystal they are predominant in the chains.

Introduction

Poly(aniline) (PANI) and its derivatives are one of the most studied conducting polymers due to their photoconductivity, electrocromic, and electronic properties, together with their higher stability in air when compared to other conducting polymers.[1−3] These amazing properties have made possible to use PANI in solar cells, displays, lightweight battery electrodes, electromagnetic shielding devices, anticorrosion coatings, and sensors.[4−6] A promising way to control and enhance the PANI bulk properties is to organize the polymeric chains in the nanometer regime.[7−10] Some ways to achieve nanostructured PANI involve the synthesis in micelar media,[11−14] the template-guided polymerization using porous surfaces,[15] and the polymerization inside the cavities of porous inorganic or organic hosts.[16−23] In the last case, the nanocomposites can enhance the electronic, mechanical, chemical, and optical properties of the conducting polymer.[23−25]

Among the different types of porous inorganic hosts, smectite clays have received great attention when the PANI confinement is desirable.[26] Clay minerals such as montmorillonite (MMT) are layered silicates, able to exchange cationic ions and intercalate neutral molecular species between the interlayer regions. There are several studies reported in the literature concerning the PANI−MMT nanocomposites.[27−34] Using mainly FTIR and EPR techniques, the formation of emeraldine salt form of PANI (PANI−ES) between the layers is proposed.[30−33]

Some others conducting polymers have been synthesized in the nanospace of the clay interlayers, such as poly(pyrrole),[35−39] poly(*o*-methoxyaniline),[40] poly(2-ethynylpyridine),[41] and poly(thiophene).[39,42] Although significant progress has been made in developing these nanocomposites, more research is necessary to characterize the structure of intercalated conducting polymers and to determine the main factors that can be controlled in the synthesis of these materials.[24]

Our group is interested in monitoring the polymerization of aromatic amines and diamines intercalated into clays and characterize the structure of the intercalated polymers through spectroscopic techniques. Resonance Raman scattering is one of the most powerful techniques in the structural investigation of conducting polymers, since it is possible to select each chromophoric segment present in the polymeric chain.[43] In the case of PANI, resonance Raman effect permits to monitor modifications in its chain units after solvent and thermal treatments.[44−46]

With the use of resonance Raman technique, we have demonstrated, in a preliminary work, that the structure of intercalated PANI in PANI−MMT nanocomposites is different from that of the free polymer, also showing benzidine (1,4-diaminebiphenyl) and N=N segments.[34] Recently, we have shown that free poly(benzidine) and its nanocomposite with MMT have similar structure.[47]

The goals of this work are to investigate the aniline polymerization reaction when intercalated between clay

[†] Universidade de São Paulo.
[‡] Universidade Estadual de Campinas.

10.1021/ma049054+ CCC: $27.50
Published on Web 11/12/2004

layers and also to characterize the dried powder isolated after reaction. In situ UV−vis−NIR, micro-Raman, and in situ small-angle X-ray scattering (SAXS) were used to monitor the polymerization of aniline intercalated into MMT. The characterization of powdered poly(aniline)−MMT nanocomposites was performed by X-ray diffraction (XRD), scanning electronic microscopy (SEM), resonance Raman (RR), FTIR, X-ray photoelectron (XPS), and X-ray in the N K-edge absorption (XANES) spectroscopies.

Experimental Section

(a) Preparation of Polymer−Clay Nanocomposite by in Situ Polymerization. Swy-2 montmorillonite (MMT, from the Clay Minerals Repository) was treated with sodium chloride and size fractionated to obtain the homoionic Na^+ form, free of main impurities.

The experimental procedure for intercalated aniline in MMT was adapted from ref 33. A total of 230 mL of an aqueous suspension of 2.6 g of MMT was thermostatized at 80 °C and then slowly dropped into 20 mL of a stirred aqueous solution, containing 0.16 mol/L of aniline (Merck, previously distillated under vacuum) and 0.30 mol/L of HCl (Merck). After stirring for 6 h at 80 °C, the suspension was filtered, and the anilinium-MMT form (An^+-MMT) was washed with deionized water until the excess of An^+ was eliminated. The An^+-MMT material was dried under dynamic vacuum and kept in a desiccator.

The An^+-MMT polymerization was conducted in two pH conditions: (a) at pH 2, adjusted by addition of aqueous HCl solution, and (b) at pH 5, the natural value of the aqueous suspension containing An^+-MMT and ammonium persulfate.

2.6 g of An^+-MMT solid was resuspended in 100 mL of deionized water, and 20 mL of suspension was used in the polymerization experiment as follows: deionized water was added to the suspension up to the final volume of 100 mL; the pH was adjusted to 2 by the addition of 1 mol/L aqueous HCl solution. Afterward, 1 mmol of ammonium persulfate (MERCK) was added, and the suspension was stirred for 24 h at room temperature. The suspensions were filtered, and the isolated dark green solids were dried under dynamic vacuum and stored in a desiccator. The elemental analyses (C, H, N) of the samples show that the An^+ concentration in An^+-MMT is about 3.5 g/100 g, and the amounts of polymer in PANI−MMT are approximately 2 g/100 g and 2.8 g/100 g for composites prepared at pH 2 and pH 5, respectively.

(b) Preparation of Poly(aniline) Forms. The emeraldine salt and base forms of PANI (PANI−ES and PANI−EB, respectively) were prepared according to the procedure described by Mac Diarmid et al.[48] The pernigraniline base form (PANI−PB) was prepared through oxidation of PANI−EB, following the procedure described in the literature.[49]

(c) Instrumentation. Resonance Raman spectra at 632.8 nm exciting radiation (from He−Ne laser, Spectra Physics, model 127) at 457.9, 488.0, and 514.5 nm exciting radiation (from Ar^+ laser Omnichrome model 543-AP) and also at 782.0 nm exciting radiation (from Solid State Laser) were recorded in a Renishaw Raman imaging microscope (system 3000), containing an Olympus metallurgical microscope and a CCD detector. Each laser beam was focused on the sample in a roughly 1 μm spot by a ×80 lens. Laser power has always been kept below 0.7 mW at the sample to avoid sample degradation.

Raman data, during the intercalated anilinium polymerization, were obtained by taking samples from the reaction bath at different times. These samples were roughly dried in air (ca. 15 min) over a microscopic slide, and then the spectra were acquired. FT-Raman spectra of solid samples were recorded in an RFS 100 FT-Raman Bruker spectrometer, using the 1064.0 nm radiation from a Nd:YAG laser.

The Raman spectra of Janus Green B (Merck) were recorded in a Jobin-Yvon U1000 spectrometer, fitted with a photomultiplier tube (RCA C31034-A02) coupled to a photon counter (EG&G PARC). The laser lines 514.5 and 488.0 nm (from Ar^+ Coherent Innova 90-6) were used, and laser power at the sample has typically been 100 mW. A circular rotating cell was used to avoid laser degradation of the sample.

The FTIR spectra were obtained by using a BOMEM MB-100 instrument with a resolution of 4 cm^{-1}, and the samples were dispersed in KBr pellets. The UV−vis−NIR spectra were obtained in a Shimadzu UVPC-3101 scanning spectrophotometer, using an integration sphere attachment. The XRD patterns of nanocomposite films were obtained in a Phillips MPD-1880 diffractometer, using Cu Kα radiation.

The XPS measurements were done by using characteristic Kα radiation from an Al anode to excite the samples and a 100 mm mean radius hemispherical analyzer operating with a constant passing of energy of 44 eV, resulting in a 1.6 eV fwhm for the Au 4f line. A small quantity of each sample was pressed between two stainless steel plates to form a thin conglomerate fixed to the sample holder with double-faced conducting tape. The analyses were done at a base pressure of 5×10^{-9} mbar, and charging effects were corrected by shifting the spectra, so that the C 1s line was at 284.6 eV.

The small-angle X-ray scattering (SAXS) experiments were conducted at the National Synchrotron Light Laboratory (LNLS), Campinas, Brazil, by using a monochromatic X-ray beam ($\lambda = 1.488$ Å), which also focuses the beam horizontally, and a position-sensitive X-ray detector to record the scattering intensity. The in situ SAXS monitoring of An^+-MMT polymerization (a total of 0.52 g of An^+-MMT solid has been resuspended in 100 mL of deionized water) was done by using a cell with mica windows.[50] The parasitic scattering intensity (mainly produced by the cell windows) was subtracted from the total experimental intensity. The SAXS curves were normalized with respect to (i) the decreasing intensity of the incoming synchrotron beam and (ii) the SAXS intensity produced by solvent (water) has been measured and subtracted from the total scattering intensity before the analysis.

The XANES spectra were obtained by using the facilities of the National Synchrotron Light Laboratory (LNLS), Campinas, Brazil. The spherical grating monochromator beamline (the spectral resolution $E/\Delta E$ of spherical grating is better than 3.000) has a focused beam of, roughly, 0.5 mm^2 spot, and the spectra were recorded in total electron yield detection, with the sample compartment pressure at 10^{-8} mbar. Measurements were done with the sample surface normal to the beam. All energy values in the N K-edge spectra were calibrated by using the first resonant peak in the N K-edge XANES spectrum of potassium nitrate.[51] The used standard compounds have been phenazine (Merck), phenosafranin (Aldrich), Janus Green B (Merck), oxazine (Aldrich), Nile Blue (Merck), Titangelb (Titan Yellow/Merck), Congo Red (Merck), Methyl Orange (Merck), Gentian Violet (Merck), *N,N′*-diphenyl-1,4-phenylenediamine (Merck), and hidrazinium dichloride (BDH).

SEM images of the samples, recovered by 16 nm of sputtered gold film, were recorded through a low-vacuum scanning electron microscope (SEM, JSM-5900LV) and operated with a high-tension voltage of 10 kV.

Results and Discussion

The An^+-MMT polymerization, using persulfate anions as oxidant, has been conducted in two pH conditions: (a) at pH 2, the experimental condition normally used to obtain free PANI,[48] and (b) at pH 5, the natural value of the aqueous suspension containing An^+-MMT and ammonium persulfate. The last condition has been used because the interlayer in smectite clays, such as MMT, is very acidic,[52] which could promote the PANI formation in the protonated form (i.e., PANI-ES), making the external acidity unnecessary.

Figure 1 shows the in situ UV−vis−NIR spectra of aqueous suspension of anilinium-MMT (An^+-MMT) at pH 2 recorded at different polymerization times. Significant spectral changes have occurred during the polymerization: after 2 h, the bands at 750 and 440 nm grew and reached their maximum at 4.5 h, while the

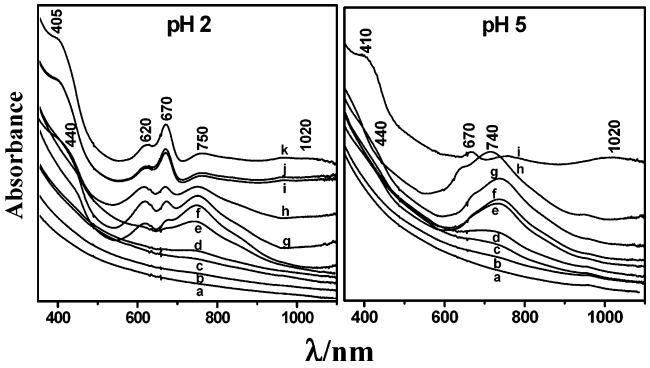

Figure 1. In situ UV−vis−NIR spectra of aqueous suspension of An^+-MMT at pH 2 (A) and pH 5 (B) after the addition of the oxidant agent. Recorded times (in h): a, 0; b,-0.5; c,-1; d, 2; e, 2.5; f, 3.5; g, 4.5; h, 5; i, 18.5; j, 20; k, 22.

bands at 670 and 620 nm started to appear after 3.5 h and reached their maximum intensities after 18.5 h. There was a continuous shift of the band at 440−405 nm with time. The absorption at 750 nm is a characteristic band of the radical cation of PANI-ES, formed by head-to-tail coupling of the anilinium radical cations.[53] The band at 440 nm has been attributed to this species or to benzidine dication, formed by tail-to-tail coupling reactions of anilinium radical cations.[54,55] The correct assignment will be elucidated by resonance Raman data.

The bands at 670 and 620 nm are not observed in the characteristic free PANI UV−vis spectrum and indicate the presence of new chromophoric segments in the intercalated polymeric structure. The tail (ca. 1020 nm) of the band localized in the near-IR appeared after 4.5 h and reached its maximum intensity after 18.5 h. This tail has been assigned to delocalized free charge carriers present in secondarily doped PANI[56] and poly(diphenylamine), PDPA,[46] and indicates that the nanocavities of clay can impose an extended conformation on the intercalated polymeric chains. The evolution of the in situ UV−vis−NIR spectra for the polymerization at pH 5 was similar to that at pH 2, but the relative intensity of the band at 670 nm was lower than the one observed in the spectra at pH 2, indicating that the formation of the new chromophoric segments are favored in more acidic medium. At this point, it is important to emphasize that at external pH 5 the polymerization also occurs.

Another way to monitor the polymerization of An^+-MMT is by resonance Raman spectroscopy. Figure 2 shows the resonance Raman (RR) spectra for two exciting radiations and the corresponding optical images for different polymerization times. In the initial stages (ca. half an hour), for both pH conditions, the samples were heterogeneous (see images in Figure 2) and the sample dark points have RR spectra, while the clear points present high fluorescence due to MMT.

The RR spectrum excited at 632.8 nm radiation presents characteristic bands of PANI-ES radical cation (at 1167, 1318/1339, and 1625 cm^{-1}) and dication (at 1481 and 1582 cm^{-1}).[57] These data confirm that the band at 750 nm in the UV−vis−NIR spectra of the early stages of the polymerization is due to this kind of radical cation segment. However, the RR spectrum excited at 488.0 nm wavelength is not the characteristic spectrum of free PANI-ES at the same exciting wavelength. The bands at 1211, 1370, 1455, and 1608 cm^{-1} can be assigned to the benzidine dication, formed by tail-to-tail coupling reactions.[58,59] Since benzidine dication bands were enhanced at 488.0 nm exciting wavelength, the electronic band at 440 nm, observed in the in situ UV−vis−NIR spectra of the early stages of the polymerization, can be attributed to this dication species. These results indicate that two kinds of coupling reactions have occurred simultaneously and that they are the same for both pH conditions. The samples become homogeneous after ca. 12 h (see Figure 2), and the RR spectra at the two exciting wavelengths are completely different from those obtained at the early stages of polymerization and stayed constant along the polymerization. These spectra are different from those characteristic of free PANI-ES and from the spectra of free or confined poly(benzidine) in MMT.[47] We have recognized this material as a new type of poly(aniline)−MMT nanocomposite.[34]

For the first time, SAXS was used to monitor the evolution of the basal spacing of clay during the intercalated anilinium polymerization. It is well-known that the degree of clay swelling in water depends on the concentration of clay, the nature of the interlayer cation, and the layer charge density.[60] Figure 3 shows the SAXS data obtained for the An^+-MMT suspension at two pH conditions for different times, after the addition of ammonium persulfate.

A broad peak has been observed at ca. $2\theta \sim 4.5°$, which confirms that the clay concentration has not been enough to delaminate the clay and that the basal spacing is about 18.8 and 19.3 Å in pH media 2 and 5, respectively. Considering the clay thickness of 9.6 Å, the gallery height is 9.2 and 9.7 Å. The SAXS data indicate that the water forms three layers of molecules inside the MMT galleries.[61] So we can visualize a heavily hydrated interlayer region containing An^+ ions with lesser freedom degrees than in aqueous solution (Scheme 1). Other important information from the SAXS experiment was that the gallery height was not changed during the polymerization.

To identify the structure of the confined conducting polymer, the poly(aniline)−MMT nanocomposites were isolated and dried, and their powders were characterized by several spectroscopic techniques.

XRD has been used to confirm the intercalation of the An^+ and to obtain the gallery height of intercalated polymer as a powder. Figure 4 shows the XRD pattern of MMT clay before and after An^+ intercalation and after polymerization at the two pH conditions. The d_{001} basal spacing was of 12.8 Å (Na^+-MMT), 13.5 Å (An^+-MMT), 13.2 Å (PANI−MMT prepared at pH 2), and 14.1 Å (PANI−MMT prepared at pH 5). The changes in the basal spacing of MMT confirm the An^+ intercalation and polymerization.

Considering a clay thickness of 9.6 Å, the gallery height is of 3.6 Å (pH 2) and 4.5 Å (pH 5) for powder PANI−MMT nanocomposites. The differences between d_{001} values of PANI−MMT prepared at pH 2 and pH 5 can be associated with the differences in the hydration degree of the clay. It is worthwhile noting that the great difference between the values of interlayer distances of powder PANI−MMT nanocomposites obtained by using XRD and those measure by SAXS during the intercalated An^+ polymerization in aqueous suspension (see Scheme 1).

We have used the SEM technique to investigate the morphological aspects of PANI−MMT nanocomposites (Figure 5). It is possible to notice that the morphologies

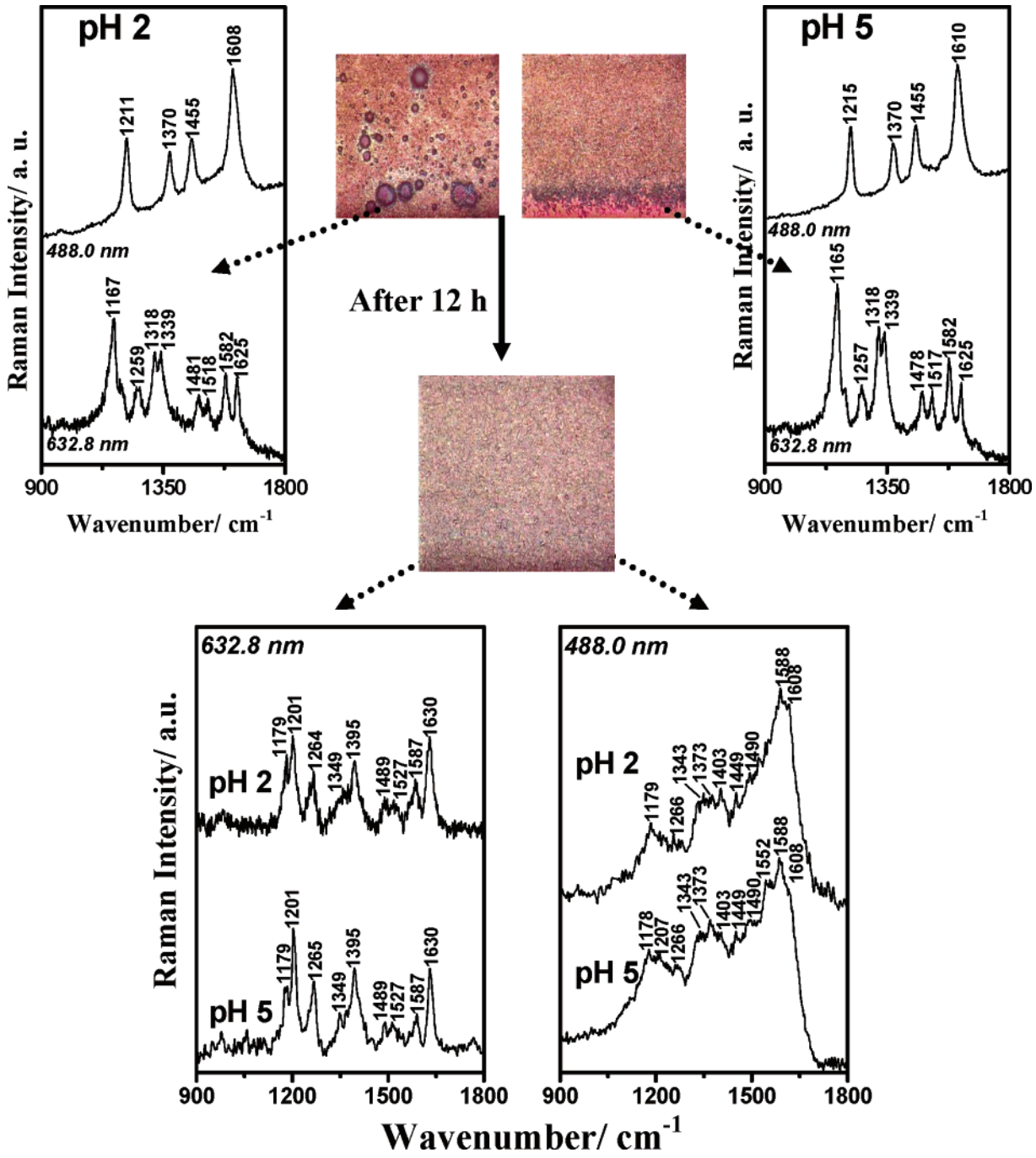

Figure 2. Resonance Raman spectra (for two exciting radiation) and optical images of dried aliquot of aqueous suspension of An^+-MMT recorded at different times after the addition of the oxidant agent: A and B, after 0.5 and 12 h.

of PANI−MMT nanocomposites (images C and D) are similar to that of the clay (image A), but very different from that of free PANI (image B). This result shows that the polymerization occurs mainly between the clay layers, thus corroborating the XRD data.

Figure 6 shows the FTIR spectra of Na^+-MMT, An^+-MMT, free PANI-ES, and PANI−MMT prepared at pH 2 and pH 5. As can be seen, the clay bands dominate FTIR spectra (ν_{Si-O} at ca. 1044 cm^{-1}), making the analysis of this spectral region difficult. In the An^+-MMT spectrum the band at 1497 cm^{-1} can be assigned to the ν_{C-N} stretching, while bands at 2860 and 2925 cm^{-1} can be attributed to the ν_{N-H} stretching modes of the NH_3^+ group,[62] confirming the presence of An^+ in the MMT clay.

Comparing spectra D and E (PANI−MMT nanocomposites) to that of the free PANI−ES, it is noticed that the bands at 1239, 1300, 1472, and 1556 cm^{-1} in the last spectrum have their counterpart band in D and E spectra, indicating that although the external pH are different the same kind of polymerization is occurring inside the gallery height. The absorption bands at 1635 cm^{-1} and the broad band at 3430 cm^{-1} in the Na^+-MMT spectrum have been assigned to bending and stretching modes of adsorbed water, respectively.[63] These bands are observed in the An^+-MMT and PANI−MMT prepared at pH 5 but are not seen in the spectrum of PANI−MMT prepared at pH 2. The absence of this band in the last spectrum made it possible to observe the bands at 3440 and 3527 cm^{-1}, which have their coun-

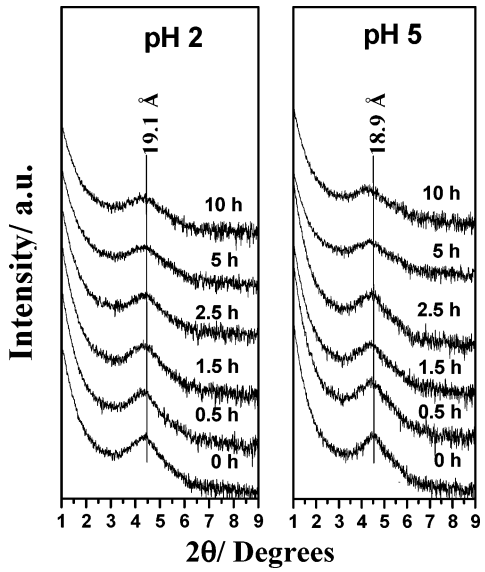

Figure 3. In situ SAXS curves of aqueous suspension of An^+-MMT at pH 2 (A) and pH 5 (B) after the addition of the oxidant agent.

terparts in the PANI−ES spectrum and are assigned to ν_{N-H} stretching modes.[57] These results show that the bands in the IR spectra of PANI−MMT nanocomposites can be associated with segments originated from head-to-tail coupling reactions.

Figure 7 shows the RR spectra of the powder PANI−MMT synthesized at pH 2 and at pH 5 for several excitation wavelengths and the RR spectra of PANI−ES for comparison purposes. Some notable spectral differences are observed in the RR spectra of PANI−MMT nanocomposites excited at 632.8 nm in relation to the PANI−ES spectrum excited at the same wavelength.

In a preliminary work,[34] the bands at 1179, 1201, 1264, 1347, and 1390 cm^{-1} in the spectrum of PANI−MMT were associated with the bands at 1175, 1200, 1270, 1320, and 1380 cm^{-1} observed in the spectra of poly(diphenylamine), PDPA, excited at 632.8 and 514.5 nm. This correspondence has been attributed to the presence of radical and dication segments of benzidine in the structure of PANI−MMT, indicating that intercalated anilinium radical cation species are involved in a tail-to-tail coupling.[64] Also in the previous communication, the weak band at 1449 cm^{-1} in the spectrum of PANI−MMT nanocomposite excited at 488.0 nm was attributed to $\nu_{N=N}$ stretching mode, in comparison with other azo compounds.[34] This band can also be seen in the spectra of the nanocomposites excited at 514.5, 488.0, and 457.9 nm wavelengths (Figure 7) and in the spectrum excited at 488 nm after 12 h of polymerization (Figure 2). This observation reinforces that, during the synthesis, there are head-to-head coupling reactions and azo bonds have been formed. The band at 1449 cm^{-1} was also observed in the Raman spectra of free and intercalated poly(benzidine) into MMT.[47]

Nevertheless, in the preliminary study, some spectral features have not been completely explained, such as (i) the new bands at 620 and 670 nm in the UV−vis−NIR spectra of PANI−MMT nanocomposites are not observed in the spectrum of free PANI and PDPA; (ii) the high relative intensities of the bands at 1201 and 1264 cm^{-1} in the PANI-MMT Raman spectrum excited at 632.8 nm, which are not expected, since these bands are very weak in the PDPA spectrum at this exciting wavelength;[46] (iii) the slight mismatch in the frequency between the corresponding band in the PANI−MMT spectrum and those of PDPA (as the bands at 1347 and 1320 cm^{-1}); and (iv) the absence of bands in the RR spectra of PDPA, which could be associate with the bands at 1412 and 1630 cm^{-1} in the spectra of PANI−MMT. These four points are puzzling features that demand further investigation.

In the spectroscopic monitoring of the thermal behaviors of free PANI and free PDPA, chromophoric segments, having high resonance Raman condition at 632.8 nm excitation wavelength, were detected. These segments were identified as phenazine and/or oxazine-like rings, formed due to cross-linking or reaction with oxygen during the thermal treatment.[46] Phenazine-like rings were also been identified in free poly(benzidine) and in poly(benzidine)−MMT.[47]

Taking all these considerations into account, we have tried to find standard compounds, having azo groups together with phenazine or oxazine-like rings in their structures, giving out vibrational and electronic signatures similar to those of the PANI−MMT nanocomposites. The best standard azo dye found was the Janus Green B (JGB). Figure 8 presents the UV−vis−NIR spectra of JGB in aqueous solution at pH 0 and in *N*-methylpyrrolidone (NMP) and the RR spectra at different excitation wavelengths of the dye in the solid state. The components at 620 and 670 nm of the broad absorption band of the dye can be observed in the last spectra of PANI−MMT in Figure 1. Also, the frequencies and relative intensities of the dye bands at 1179, 1201, 1347, 1400, and 1628 cm^{-1} in the RR spectrum at 632.8 nm exciting radiation (Figure 8B) are in good agreement with those of PANI−MMT nanocomposites at the same radiation (Figure 7). Therefore, this result indicates that a phenazine-type ring is another kind of segment present in the polymeric structure. It is worth noting that the 620 and 670 nm bands that appeared in the in situ UV−vis−NIR spectra (Figure 1) are associate with chromophoric segments (having a N=N azo bond plus a phenazine-like ring) and that these segments have only appeared after ca. 3 h of polymerization and are more evident for the composite prepared at pH 2.

Considering the vibrational data, the intercalated polymeric structure presents segments formed by head-to-tail coupling reactions of anilinium radical cations (radical cation, dication, and reduced moieties of 1,4-phenylenediamine repeat units), which are present in free PANI−ES. Also, there are segments formed by tail-to-tail coupling reactions of anilinium radical cations (dication of benzidine repeat units), together with azo bonds and phenazine-like segments. These segments have been presented in Scheme 2.

To understand the variation of PANI−MMT Raman spectra with the exciting radiation (Figure 7), it is necessary to consider all the resonance Raman conditions of each segment in the polymeric chains. At 632.8 nm, the bands of phenazine-like rings are in resonance, but when the wavelength of the exciting radiation increases or decreases, the spectra of PANI−MMT nanocomposites become more similar to those of free PANI−ES. For 1064 and 457.9 nm exciting wavelengths (Figure 7), the majority of the bands in the spectra of the nanocomposites has their counterpart in the spectra of free PANI−ES, which means that, at these

Scheme 1. Schematic Representation of Intercalation and Polymerization Processes of An^+ Ions into MMT Galleries

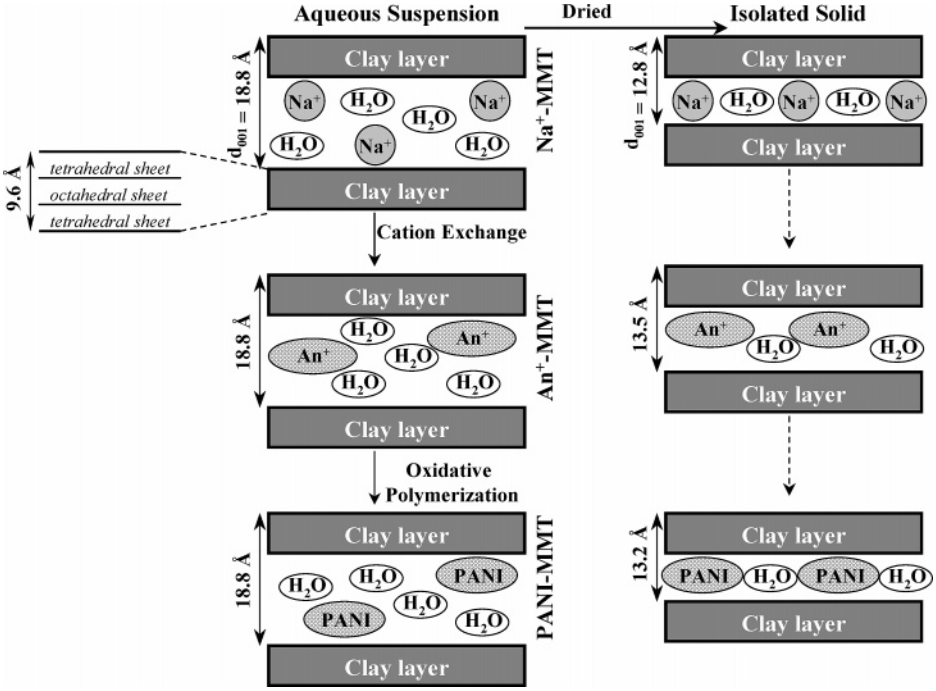

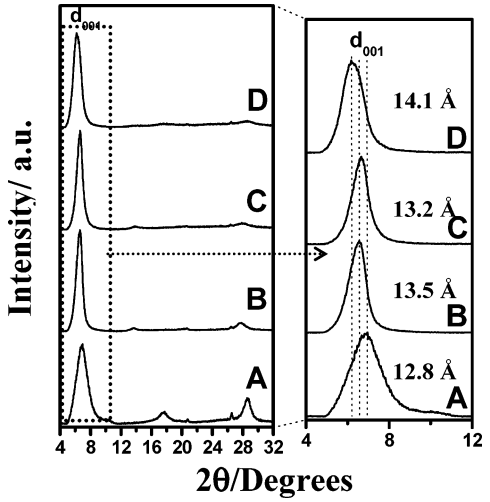

Figure 4. X-ray diffractionpatterns of powder samples: Na^+-MMT (A), An^+-MMT (B), PANI−MMT prepared at pH 2 (C), and PANI−MMT prepared at pH 5 (D).

exciting wavelengths, the chromophoric segments that are in resonance condition are those present in free PANI−ES.

The PANI−MMT nanocomposites spectra at 457.9 nm excitation wavelength show bands at 1191 and 1613 cm^{-1}, which can be assigned to the vibrational modes of benzene rings of the reduced 1,4-phenylenediamine repeat units,[57] while the bands at 1328, 1367, and 1623 cm^{-1}, in the PANI−MMT spectra at 1064 nm, can be assigned to radical cation of the 1,4-phenylenediamine repeat units.[57] It is worth emphasizing the high relative intensities of the bands at 1495 and 1582 cm^{-1} in the PANI−MMT spectra at 1064 nm, which are characteristic dication bands of PANI−ES, and suggesting a great amount of this segment in the confined polymeric chain.

The observed Raman bands of PANI−MMT nanocomposite, prepared at pH 2, and their counterpart bands in the spectra of PANI−ES, PDPA, and JGB dye are presented in Table 1. A tentative assignment of the bands based on those of PANI−ES,[57,65,66] of phenazine,[67−71] and of azobenzene[72] is also presented. No attribution of the vibrational bands of JGB was found in the literature.

A technique that can be used to distinguish different types of nitrogen is the X-ray absorption in the N K-edge (XANES).[73] Henning et al.[74−76] have demonstrated the viability of using the XANES technique to characterize the different oxidation states of nitrogen atoms in the PANI chain. To use this spectroscopy to improve our knowledge of the polymeric chains in PANI−MMT nanocomposites, XANES spectra of compounds with nitrogen in different chemical states must be measured. As can be seen in Figure 9, the energy values change very little with the type of nitrogen atoms (see structural formula in Scheme 3), although a general correlation between band values and the kind of nitrogen atoms can be taken from the XANES spectra. The spectra of the compounds, having an imine nitrogen ring, =N−, present a low-energy band in the 398.2−398.3 eV (spectra A−E of Figure 9). For compounds having positively charged imine nitrogen in the phenazinic ring or in quinoid segments, $\rangle N^+=$, a band appears in the 399.4−399.6 eV (spectra B−E and K). In azo dyes spectra (C, F−H), there is a band in the 398.7−398.9 eV that can be assigned to −N=N− azo bonds.

Following the assignment proposed by Henninget al.,[76] the band in the 400.4−400.7 eV, observed in spectra A−C, can be assigned to delocalized imine groups. In compounds having amine nitrogen, −NH−, there is a band in the 401.8−402.7 eV. In the spectrum of hidrazinium dichloride, the band at 404.6 eV can be assigned to protonated hydrazinic nitrogens, $N_2H_6^{2+}$. Table 2 lists the bands of the standard compounds, and a tentative assignment of the bands is presented.

Figure 10 shows the XANES spectra of PANI−MMT nanocomposites synthesized at pH 5 and pH 2 (spectra D and E, respectively) and the XANES spectra of free PANI−EB, PANI−PB, and PANI−ES, spectra A, B, and

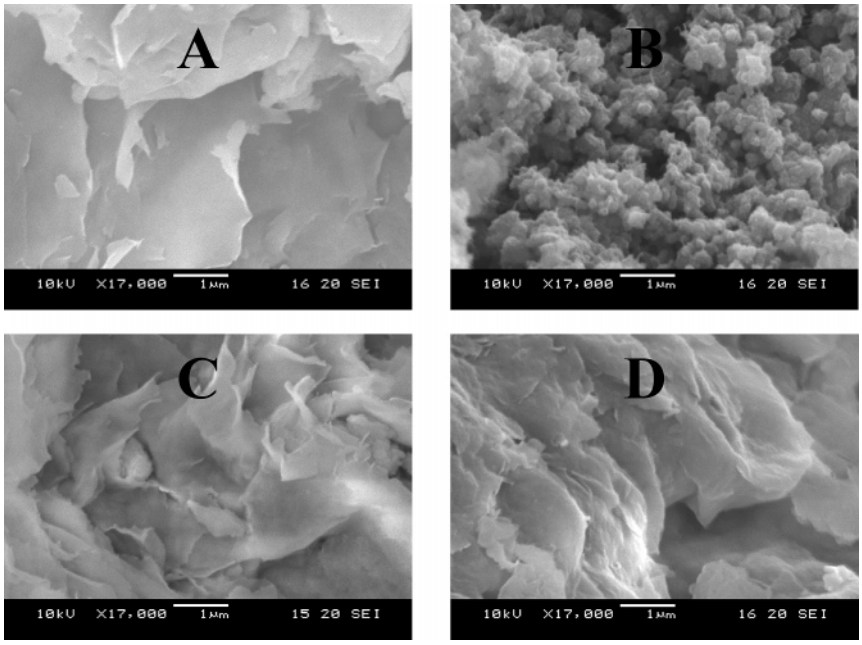

Figure 5. SEM images of samples: Na^+-MMT (A), PANI−ES (B), PANI−MMT prepared at pH 5 (C), and PANI−MMT prepared at pH 2 (D).

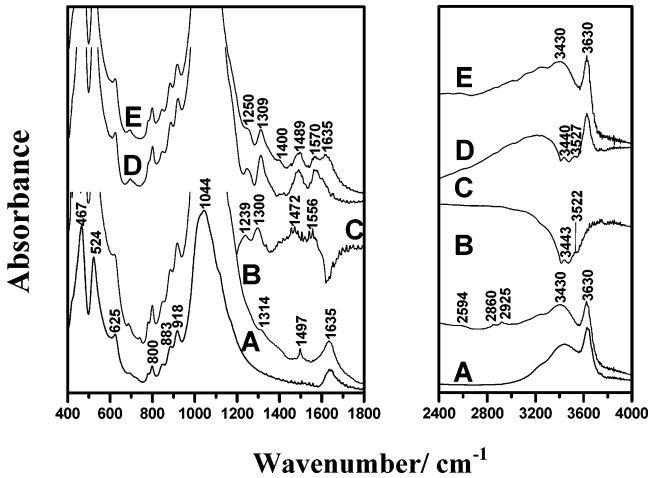

Figure 6. FTIR spectra of solid samples dispersed in KBr pellets: Na^+-MMT (A), An^+-MMT (B), PANI−ES (C), PANI−MMT prepared at pH 2 (D), and PANI−MMT prepared at pH 5 (E).

C, respectively. A tentative assignment of the peaks in the spectra of the free PANI forms based on Henning et al.[76] is also presented in Table 2. The bands at ca. 398.5 and 398.9 eV in the spectrum of PANI−MMT prepared at pH 5 and pH 2 can be assigned to −N= imine nitrogens of phenazine-like rings and to −N=N− azo bonds, respectively. This result confirms the presence of phenazine-like rings and azo bonds in the nanocomposites, corroborating the resonance Raman data. The band at 398 eV in the PANI−MMT prepared at pH 5 can be assigned to −N= imine nitrogens of quinoid segments. The band at 399.2 eV in the spectra of PANI−MMT prepared at pH 2, not resolved in the spectrum of PANI−MMT prepared at pH 5, has the counterpart band at 399.1 eV in the PANI−ES spectrum (part C in Figure 10) and can be attributed to radical nitrogens. The band at 399.9 eV can be assigned to positively charged imine nitrogens, while the bands at 400.4 and 401.9 eV can be attributed to delocalized imine and amine nitrogens, respectively. Maybe the band at 403.0 eV in the PANI−MMT nanocomposites spectra could be associated with hydrazinium nitrogens groups in the polymeric chains. However, the band at 404 eV is also observed for compounds that do not have hidrazinium nitrogens (Figure 9A−C,H,J).

X-ray photoelectron spectroscopy has been largely used for characterizing the nitrogen oxidation states of PANI.[77−80] Figure 11 shows the characteristic N 1s XPS spectra of PANI−EB and PANI−ES. The lines at 398.1, 399.3, and 400.8 eV in the PANI−EB spectrum can be assigned to imine (=N−), amine (−NH−), and radical ($-N^{\bullet+}=$) nitrogens, respectively. The lines at 399.2 and 401.3 eV in the PANI−ES spectrum are due to amine and radical nitrogens, respectively.[77] The spectrum of PANI−MMT nanocomposite prepared at pH 2 (Figure 11C) presents three lines at 399.2, 400.8, and 402.8 eV. The weak line at 399.2 eV can be assigned to the amine nitrogens and the 400.8 eV to radical nitrogens, while the line at 402.8 eV, which does not have a counterpart in the PANI−EB and PANI−ES spectra, can tentatively be assigned to protonated amine nitrogens.[78,79] The presence of radical cations in the PANI−MMT nanocomposite samples has also been shown by EPR measurements.[34]

It is known that in the XPS signal the majority of the information comes from the first three atomic monolayers, which means that only the polymeric chains on the external surface or on the edge of clay crystal contribute to the XPS signal of PANI−MMT nanocomposite. Therefore, the low values of N/Si ratio (0.026, the Si peak has not been shown) obtained for the PANI−MMT suggest that only a small fraction of polymer is on the external clay surface, which is in agreement with the SEM images (Figure 5).

The absence of peaks in the PANI−MMT XPS spectrum which can be assigned to nitrogen atoms of the phenazine-like rings and azo units suggests that these segments are not present in the polymeric chains on the external surface (basal surface and the edges) of the clay. Some reason for the preferential localization of chains, having head-to-tail segments on the basal surface or on the edges of the clay particles, can be the

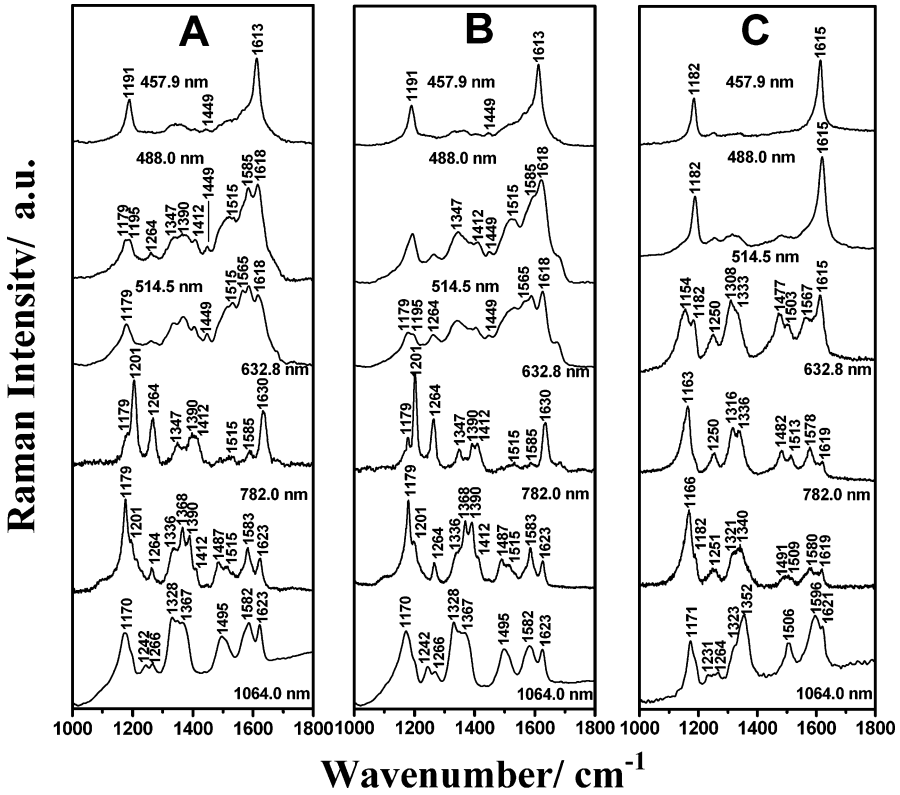

Figure 7. Resonance Raman spectra of powder samples of PANI−MMT prepared at pH 5 (A), PANI−MMT prepared at pH 2 (B), and PANI−ES (C), obtained at several excited radiations.

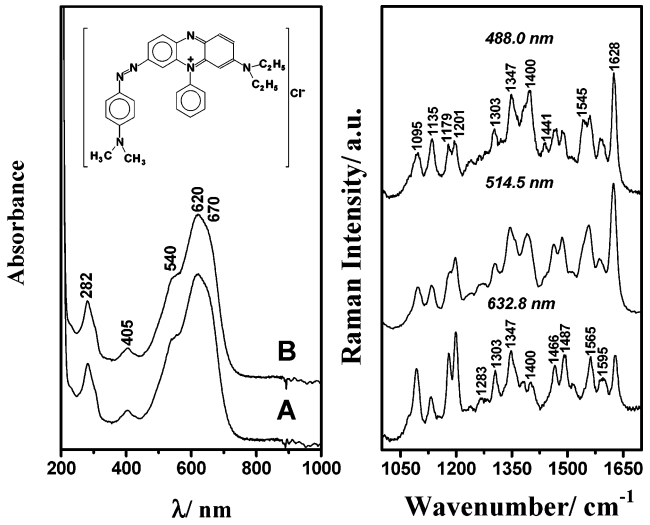

Figure 8. UV−vis-NIR spectra of solutions of Janus Green B azo dye in NMP (A), aqueous acidic solution (B), and Resonance Raman spectra of Janus Green B azo dye in a solid state obtained at several exciting radiations. The dye molecular structure is also shown.

easier access of the oxidizing agent. This observation is consistent with spectroscopic data at the initial stages of An^+-MMT polymerization, which show that PANI−ES is formed and phenazine-like rings plus N=N bonds are absent.

From the characterization results, it has been possible to state that the intercalated polymeric chain is different from that of PANI−ES. The formation of these new structures, not common in the absence of the clay, could be a consequence of the confinement of the monomers. The An^+ can assume some different orientations inside the gallery height and the electric field between the sheets can change the An^+ electronic distribution. These effects, together with smaller degree of freedom for An^+ imposed by the gallery height (ca. 9.5 Å), are important factors to be considered when trying to rationalize the difference between the free and the confined monomer polymerization mechanisms.

In Scheme 2A, the possible parallel reaction pathways for the free aniline polymerization in acidic medium giving PANI−ES are presented. The head-to-tail coupling reactions occur with higher frequency than the others.[64] Only in strong acidic medium are the benzidine and its dication the major product.[54] The absence of hydrazo segments has been attributed to the rearrangement that *N,N′*-diphenylhydrazine undergoes in acidic medium, leading to benzidine.[64]

The ensemble of spectroscopic data, obtained in this study, allows us to infer that PANI-ES-like chains are present in the structure of PANI−MMT nanocomposites. Benzidine segments have also been detected, and its formation can be explained by considering the acidity inside the gallery. The electronic absorptions at 620 and 670 nm indicate that azo bond and phenazine-like segments are present in the confined polymeric chain (see Scheme 2B). It is worth emphasizing that only after 3 h of polymerization these chromophoric segments have been detected, which suggests that benzidine segments can participate in its formation. The experimental evidence of this participation is the decrease of the characteristic RR spectrum of benzidine dication after this polymerization time. Considering all these results, one possible reaction pathway for their formation is presented in Scheme 2B.

We have mentioned above some possible reasons responsible for the intercalated PANI formation with distinct structure compared to the free polymer. Several clay properties should be important when a polymeri-

Scheme 2. Schematic Representation of Probable Chromophoric Segments Present in Intercalated PANI Chains

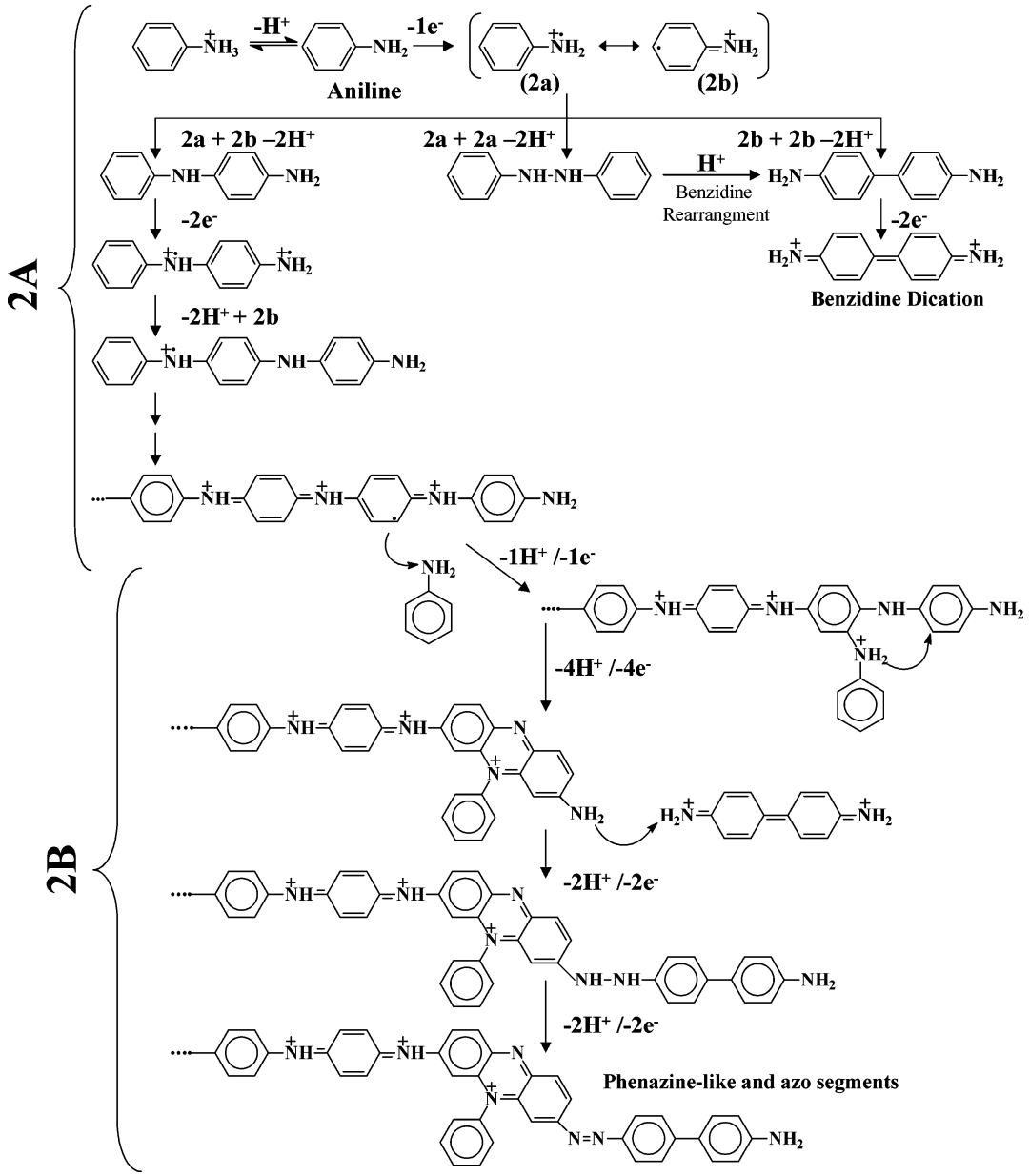

zation reaction is considered: Bronsted and Lewis acidity, layer charge density, chemical composition, swelling ability, isomorphic substitution (tetrahedral or octahedral sheet), redox properties of cations in interlayer and intralayer region, purity, etc. External parameters such as pH, oxidant agent, ionic strenght, solvent, and temperature should also influence the polymerization pathways. We have only used Swy-2 montmorillonite in the Na^+ form as precursor, but other clays could be investigated in order to stress the role of host properties in aniline condensation in the galleries. For example, recently a very interesting work was reported about the influence of a set of clays with different iron content and localization in the pyrrole adsorption and polymerization.[36] In the present study, some external parameters (as pH and polymerization time) were varied, but other ones could be investigated in order to get the influence in the final characteristic of the PANI−clay systems.

The determination of the polymeric structure of PANI−MMT nanocomposites is important considering the many possible applications of these materials. It is expected that the conducting polymer intercalation in matrices as clays produce a better chain alignment or orientation compared to the bulk polymer in order to enhance, for example, the electric conductivity.[23,29] (Other properties such as thermal and mechanical can also be enhanced.[37]) The literature has show that in general the intercalation of electroactive polymers (in clays and some other hosts) produces materials with a lower electrical conductivity than the nonconfined polymer.[7,26,28] In a previous work[34] we showed that the PANI−MMT electrical conductivity is about 10^{-3} S cm^{-1}, a value similar to those reported in the literature.[33] Some authors have claimed that the particles containing intercalated conducting polymer could be not connected among them, consequently decreasing the electrical transport.[7,33,35] So the electrical response could be increased if an excess of polymer outside the particles is present. Probably, there is a monomer/host ratio where the compromise between the confinement effect (i.e., polymer chain alignment) and the electrical contact of the particles is maximized. Other reasons can be pointed out for the low conductivity of intercalated

Table 1. Raman Bands in PANI−MMT Spectra and Their Associated Bands in PANI−ES, Janus Green B Azo Dye, and PDPA

exciting wavelengths (nm)						
457.9	488.0	514.5	632.8	782.0	1064.0	tentative assignt
			1630			Ph ring[b]
	[1628][a]	[1628]	[1628]			
				1623	1623	νC−C (SQ)[c]
			(1619)	(1619)	(1621)	
1613	1618	1618				νC−C (B)[c]
(1613)[a]	(1615)	(1615)				
	1585	1585	1585	1583	1582	ν_{C-C} (Q)[c]
			(1578)	(1580)	(1596)	
		1565				ν_{C-C} (SQ)
		(1567)				
	1515	1515	1515	1515		β_{N-H}
		(1503)	(1513)	(1509)		
				1487	1495	ν_{C-N} (Q)
		(1477)	(1482)	(1491)	(1506)	
1449	1449	1449				$\nu_{N=N}$
	[1441]					
	1412	1412	1412	1412		Ph ring
	[1400]	[1400]	[1400]			
	1390	1390	1390	1390		ν_{C-C} BZ^{2+} [d]
{1380}[I]	{1380}	{1380}	{1380}			
	1347	1347	1347			Ph ring
	[1347]	[1347]	[1347]			
				1336/1368	1330/1367	ν_{C-N} (SQ)
	(1308/1333)	(1308/1333)	(1316/1336)	(1321/1340)	(1323/1352)	
	1264	1264	1264	1264	1266	ν_{C-N} (B),
	(1250)	(1250)	(1250)	(1251)	(1264)	Ph ring
	[1303]	[1303]	[1303]			
					1242	
					(1231)	
			1201	1201		Ph ring
	[1202]	[1202]	[1201]			
1191	1195					β_{C-H} (B)
(1182)	(1182)	(1182)		(1182)		
	1179	1179	1179	1179		Ph ring
	[1179]	[1179]	[1179]			
					1170	β_{C-H} (Q)
			(1163)	(1166)	(1171)	
		(1154)				β_{C-H} (SQ)

[a] Standard compounds bands: (...) PANI−ES; [...] JGB; {...} PDPA. [b] Ph: phenazine ring vibrations. [c] SQ, B, and Q: abreviations of semiquinone, benzenoid, and quinoid segments of PANI−ES. [d] BZ^{2+}: abreviation of dication benzidine.

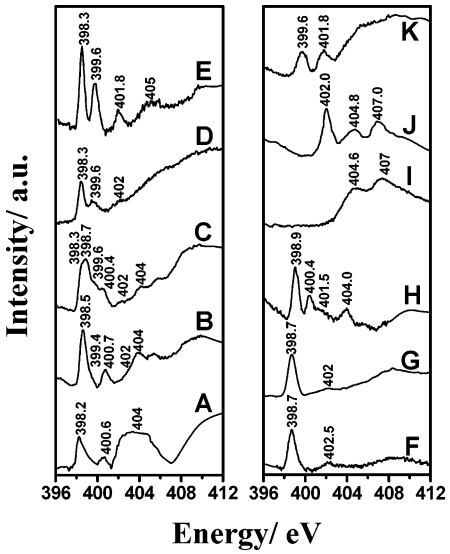

Figure 9. N-K XANES spectra of solid samples of phenazine (A), phenosafranin (B), Janus Green B (C), Nile Blue (D), oxazine (E), Congo Red (F), Methyl Orange (G), Titangelb (Titan Yellow) (H), hidrazinium chloride (I), *N*,*N*′-diphenyl-1,4-phenylenediamine (J), and Gentian Violet (K).

electroactive polymers. For PANI−clay composites in particular, the low electrical response was attibuted to the increase in the charge carriers localization and decrease in the conjugation length of the organic chain.[23] The data reported in this paper show that other parameters could be also considered. Perhaps the appearance of chromophoric groups as phenazine and azo in the PANI carbonic chain decreases the length of conjugation. At this time it is not possible to evaluate exclusively the role of the chromophoric segments observed in PANI−MMT in its electrical conductivity since other parameters (the poor electrical contact among the particles for example) can be operating. Our results have shown that to overcome the formation of such groups it is necessary to control the polymerization time and the pH of the suspension (and/or the clay acidity). However, as discussed above, other clay properties and external parameters should be systematically investigated. We believe that the data here reported are important to guide future works focusing on the preparation of PANI−clay composites with interesting properties.

Conclusions

The oxidative polymerization of anilinium in MMT occurs in a gallery height having about 9.5 Å, and the initial products are PANI−ES and benzidine dications. New chromophoric segments appear as the polymerization proceeds. The electronic bands at 670 and 620 nm and an intense RR spectrum at 632.8 nm are

Scheme 3. Schematic Representation of Chemical Structures of the Standard Compounds

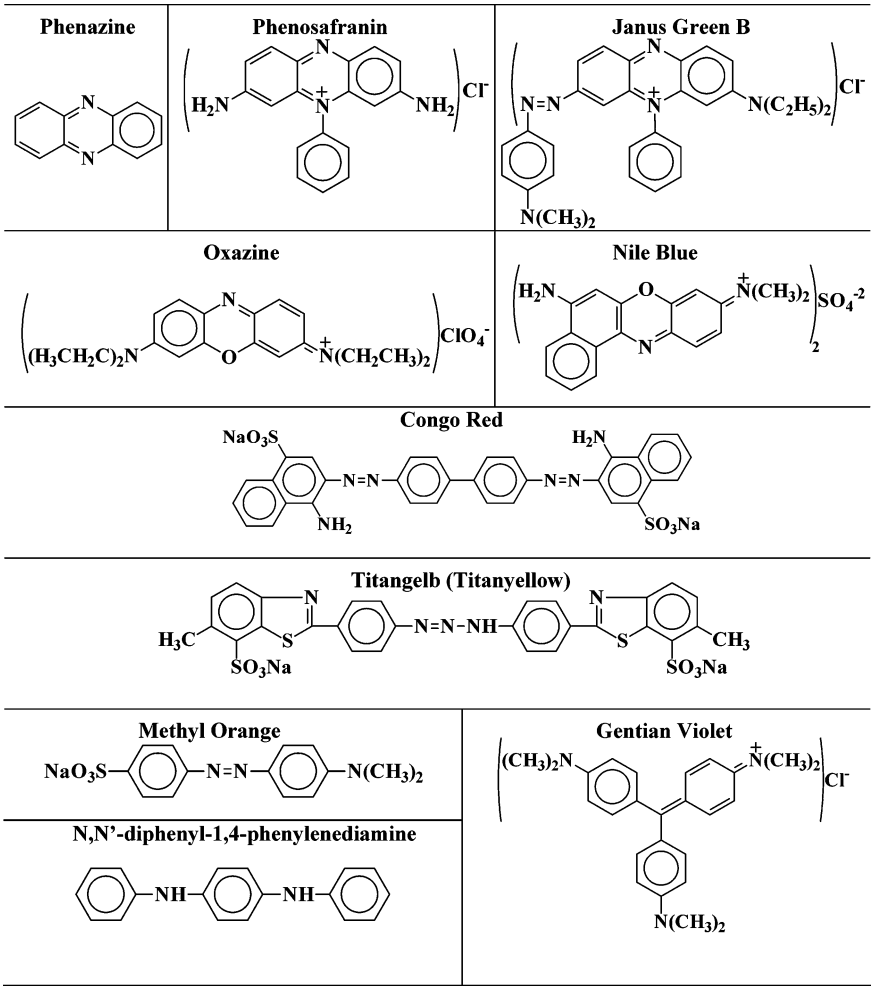

Table 2. N-K XANES Bands of Standard Compounds PANI−ES, PANI−EB, and PANI−PB

Compounds	Resonance	Energy/ eV						
	N1s→π*							
	=N− Quinoid ring	=N− Phenazinic or Oxazinic ring	-N=N-	$-\overset{+\bullet}{N}H-$	$-\overset{+}{N}=$	=N-	-NH-	$N_2H_6^{+2}$
PANI-EB	397.7	--	--	--	--	400.6	402.7	--
PANI-PB	397.7	--	--	--	--	400.6	--	--
PANI-ES	--	--	--	399.1	--	--	402.7	--
Phenazine	--	398.2	--	--	--	400.6	--	--
Phenosafranin	--	398.5	--	--	399.4	400.7	~ 402	--
Janus Green B	--	398.3	398.7	--	399.6	400.4	~ 402	--
Nile Blue	--	398.3	--	--	399.6	--	~ 402	--
Oxazine	--	398.3	--	--	399.6	--	401.8	--
Congo Red	--	--	398.7	--	--	--	402.5	--
Methyl Orange	--	--	398.7	--	--	--	402.0	--
Titangelb	--	--	398.9	--	--	400.4	401.5	--
Hidrazinium chloride	--	--	--	--	--	--	--	404.6
N,N'-diphenyl-1,4-phenylenediamine	--	--	--	--	--	--	402.0	--
Gentian Violet	--	--	--	--	399.6	--	401.8	--

fingerprints of these segments. The XRD diffraction pattern and SEM images of the powder PANI−MMT nanocomposites indicate that the polymerization occurs mainly between the clay layers. The gallery height is 3.6 and 4.5 Å for powder PANI−MMT nanocomposites prepared at pH 2 and pH 5, respectively. The IR spectra of nanocomposites present only bands due to PANI−ES-like segments. Resonance Raman, nitrogen XANES

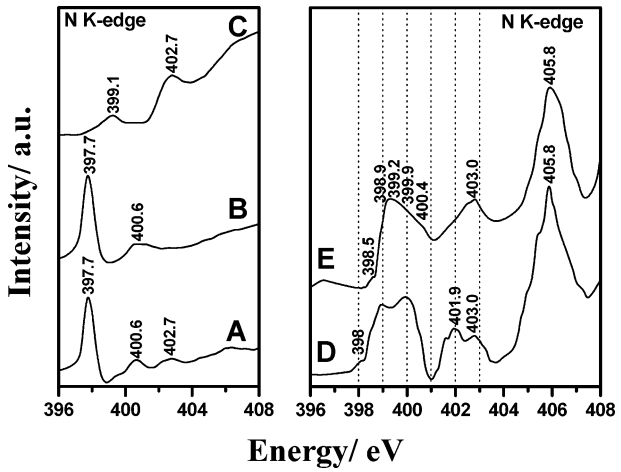

Figure 10. N-K XANES spectra of solid samples of PANI−EB (A), PANI−PB (B), PANI−ES (C), and PANI−MMT prepared at pH 5 (D) and pH 2 (E).

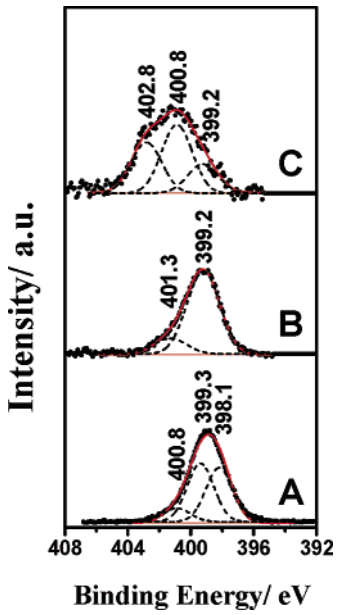

Figure 11. N 1s XPS spectra of solid samples of: PANI−EB (A), PANI−ES (B), and PANI−MMT prepared at pH 2 (C).

spectra of free PANI−ES, PANI−EB, and PANI−PB, and standard compounds have been compared to those of PANI−MMT nanocomposites, leading to the presence of PANI−ES chains, benzidine segments, azo bonds, and phenazine-like rings in the structure of confined conducting polymers. XPS technique detects only PANI−ES segments of the intercalated polymeric structure, suggesting that they are adsorbed on the external surface and/or on the edge of clay crystal.

Acknowledgment. This work has been supported by FAPESP (Brazilian agency). Fellowships from FAPESP (G.M. do Nascimento) and CNPq (M.L.A. Temperini, V.R.L. Constantino and R. Landers) are gratefully acknowledged. The authors thank the National Synchrotron Light Laboratory (LNLS/Brazil) for the use of XANES N K-edge (SGM 1026/01, 1427/02, 1432/02, and 2169/03) and SAXS (SAXS 1458/02) lines and the LME-LNLS for technical support during SEM measurements. The authors are also grateful to Miss P. M. Dias for providing the Na^+-MMT suspensions.

References and Notes

(1) MacDiarmid, A. G.; Epstein, A. J. *J. Chem. Soc., Faraday Trans.* **1989**, *88*, 317.
(2) Geniès, E. M.; Boyle, A.; Lapkowski, M.; Tsintavis, C. *Synth. Met.* **1990**, *36*, 139.
(3) MacDiarmid, A. G. *Synth. Met.* **2002**, *125*, 11.
(4) Wessling, B. *Synth. Met.* **1997**, *85*, 1313.
(5) MacDiarmid, A. G. *Synth. Met.* **1997**, *84*, 27.
(6) MacDiarmid, A. G.; Epstein, A. In *Frontiers of Polymers and Advanced Materials;* Prasad, P. N., Ed.; Plenum Press: New York, 1984; p 251.
(7) Ruiz-Hitzky, E.; Aranda, P. *Anal. Quim. Int. Ed.* **1997**, *93*, 197.
(8) Cardin, D. J. *Adv. Mater.* **2002**, *8*, 553.
(9) Thiyagarajan, M.; Samuelson, L. A.; Kumar, J.; Cholli, A. L. *J. Am. Chem. Soc.* **2003**, *125*, 11502.
(10) Huang, J.; Kaner, R. B. *J. Am. Chem. Soc.* **2004**, *126*, 851.
(11) Haba, Y.; Segal, E.; Narkis, M.; Titelman, G. I.; Siegmann, A. *Synth. Met.* **1999**, *106*, 59.
(12) Wei, Z.; Zhang, Z.; Wan, M. *Langmuir* **2002**, *18*, 917.
(13) Wei, Z.; Wan, M. *Adv. Mater.* **2002**, *14*, 1314.
(14) Kim, B.-J.; Oh, S.-G.; Han, M.-G.; Im, S.-S. *Langmuir* **2000**, *16*, 5841.
(15) Martin, C. R. *Acc. Chem. Res.* **1995**, *28*, 61.
(16) Wu, C. G.; Bein, T. *Science* **1994**, *264*, 1757.
(17) Chang, T.-C.; Ho, S.-Y.; Chao, K.-J. *J. Phys. Org. Chem.* **1994**, *7*, 371.
(18) Wu, C.-G.; DeGroot, D. C.; Marcy, H. O.; Schindler, J. L.; Kannewurf, C. R.; Bakas, T.; Papaefthymiou, V.; Hirpo, W.; Yesinowski, J. P.; Liu, Y.-J.; Kanatzidis, M. G. *J. Am. Chem. Soc.* **1995**, *117*, 9229.
(19) Zarbin, A. J. G.; De Paoli, M.-A.; Alves, O. L. *Synth. Met.* **1999**, *99*, 227.
(20) Do Nascimento, G. M.; Pereira da Silva, J. E.; Córdoba de Torresi, S. I.; Santos, P. S.; Temperini, M. L. A. *Mol. Cryst. Liq. Cryst.* **2002**, *374*, 53.
(21) Moujahid, E. M.; Dubois, M.; Besse, J.-P.; Leroux, F. *Chem. Mater.* **2002**, *14*, 3799.
(22) Cho, M. S.; Choi, H. J.; Ahn, W.-S. *Langmuir* **2004**, *20*, 202.
(23) Mehrota, V.; Giannelis, E. P. *Solid State Commun.* **1991**, *77*, 155.
(24) Vaia, R. A.; Giannelis, E. P. *MRS Bull.* **2001**, *26*, 394.
(25) Schmidt, D.; Shah, D.; Giannelis, E. P. *Curr. Opin. Solid State Mater. Sci.* **2002**, *6*, 205.
(26) Ruiz-Hitzky, E.; Aranda, P.; Serratosa, J. M. Clay-Organic Interactions: Organoclay Complexes and Polymer-Clay Nanocomposites. In *Handbook of Layered Materials*; Auerbach, S. M., Carrado, K. A., Dutta, P. K., Eds.; Marcel Dekker: New York, 2004; p 91.
(27) Feng, B.; Su, Y.; Song, J.; Kong, K. *J. Mater. Sci., Lett.* **2001**, *20*, 293.
(28) Chang, T. C.; Ho, S. Y.; Chao, K. J. *J. Chin. Chem. Soc.* **1992**, *39*, 209.
(29) Frisch, H. L.; Xi, B.; Qin, Y.; Rafailovich, M.; Yang, N. L.; Yan, X. *High Perform. Polym.* **2000**, *12*, 543.
(30) Kim, B. H.; Jung, J. H.; Kim, J. W.; Choi, H. J.; Joo, J. *Synth. Met.* **2001**, *117*, 115.
(31) Kim, B. H.; Jung, J. H.; Kim, J. W.; Choi, H. J.; Joo, J. *Synth. Met.* **2001**, *121*, 1311.
(32) Biswas, M.; Ray, S. S. *J. Appl. Polym. Sci.* **2000**, *77*, 2948.
(33) Wu, Q.; Xue, Z.; Qi, Z.; Wang, F. *Polymer* **2000**, *41*, 2029.
(34) Do Nascimento, G. M.; Constantino, V. R. L.; Temperini, M. L. A. *Macromolecules* **2002**, *35*, 7535.
(35) Kim, B. H.; Hong, S. H.; Joo, J.; Park, I.-W.; Epstein, A. J.; Kim, J. W.; Choi, H. J. *J. Appl. Phys.* **2004**, *95*, 2697.
(36) Letaïef, S.; Aranda, P.; Ruiz-Hitzky, E. *Appl. Clay Sci.*, in press.
(37) Liu, Y.-C.; Ger, M.-D. *Chem. Phys. Lett.* **2002**, *362*, 491.
(38) Faguy, P. W.; Lucas, R. A.; Ma, W. *Colloids Surf. A* **1995**, *105*, 105.
(39) Oriakhi, C. O.; Lerner, M. M. *Mater. Res. Bull.* **1995**, *30*, 723.
(40) Yeh, J.-M.; Chin, C.-P. *J. Appl. Polym. Sci.* **2003**, *88*, 1072.
(41) Liu, H.; Kim, D. W.; Blumstein, A.; Kumar, J.; Tripathy, S. K. *Chem. Mater.* **2001**, *13*, 2756.
(42) Ballav, N.; Biswas, M. *Synth. Met.* **2004**, *142*, 309.
(43) Batchelder, D. N. In *Optical Techniques to Characterize Polymer Systems;* Brässler, H., Ed.; Elsevier: Amsterdam, 1987; p 393.
(44) Pereira da Silva, J. E.; Córdoba de Torresi, S. I.; De Faria, D. L. A.; Temperini, M. L. A. *Synth. Met.* **1999**, *101*, 834.
(45) Pereira da Silva, J. E.; De Faria, D. L. A.; Córdoba de Torresi, S. I.; Temperini, M. L. A. *Macromolecules* **2000**, *33*, 3077.

(46) Do Nascimento, G. M.; Pereira da Silva, J. E.; Córdoba de Torresi, S. I.; Temperini, M. L. A. *Macromolecules* **2002**, *35*, 121.
(47) Do Nascimento, G. M.; Constantino, V. R. L.; Temperini, M. L. A. *J. Phys. Chem. B* **2004**, *108*, 5564.
(48) MacDiarmid, A. G.; Chiang, J. C.; Richter, A. F.; Sonosiri, N. L. D. In *Conducting Polymers*; Alcácer, L., Ed.; Reidel Publications: Dordrecht, 1987; p 105.
(49) Sun, Y.; MacDiarmid, A. G.; Epstein, A. J. *J. Chem. Soc., Chem. Commun.* **1990**, *7*, 529.
(50) Cavalcanti, L. P.; Kellermann, G.; Plivelic, T.; Neuenschwander, R.; Torriani, I. L. In Activity Report/National Synchrotron Light Laboratory (1997/98) Campinas, SP: Brazilian Association for Synchrotron Light Technology, 1997; p 5.
(51) Vinogradov, A. S.; Akimov, V. N. *Opt. Spectrosc.* **1998**, *85*, 53.
(52) Helsen, J. *J. Chem. Educ.* **1982**, *59*, 1063.
(53) MacDiarmid, A. G.; Huang, W. S. *Polymer* **1993**, *34*, 1833.
(54) Gospodinova, N.; Terlemezyan, L. *Prog. Polym. Sci.* **1998**, *23*, 1443.
(55) Yariv, S. Staining of Clay Minerals and Visible Absorption Spectroscopy of Dye-Clay Complexes. In *Organo-Clay Complexes and Interactions;* Yariv, S., Cross, H., Eds.; Marcel Dekker: New York, 2002; p 463.
(56) MacDiarmid, A. G.; Epstein, A. J. *Synth. Met.* **1994**, *65*, 103.
(57) Furukawa, Y.; Ueda, F.; Hyodo, Y.; Harada, I.; Nakajima, T.; Kawagoe, T. *Macromolecules* **1988**, *21*, 1297.
(58) Gao, P.; Gosztola, D.; Weaver, M. J. *J. Phys. Chem.* **1989**, *93*, 3753.
(59) Soma, Y.; Soma, M. *Clay Mineral.* **1988**, *23*, 1.
(60) Yariv, S.; Michaelian, K. H. Structure and Surface Acidity of Clay Minerals. In *Organo-Clay Complexes and Interactions;* Yariv, S., Cross, H., Eds.; Marcel Dekker: New York, 2002; p 1.
(61) Manias, E.; Panagiotopoulos, A. Z.; Zax, D. B.; Giannelis, E. P. Structure and Dynamics of Nanocomposite Polymer Electrolytes. In *CMS Workshop Lectures Electrochemical Properties of Clays;* Fitch, A., Ed.; The Clay Mineral Society: Aurora, CO, 2003; Vol. 10, p 185.
(62) Yariv, S. IR Spectroscopy and Thermo-IR Spectroscopy in the Study of the Fine Structure of Organo-Clay Complexes. In *Organo-Clay Complexes and Interactions;* Yariv, S., Cross, H., Eds.; Marcel Dekker: New York, 2002; p 345.
(63) Madejova, J.; Komadel, P. *Clay Clay Mineral.* **2001**, *49*, 410.
(64) Wei, Y.; Harihoron, R.; Patel, S. A. *Macromolecules* **1990**, *23*, 758.
(65) Louarn, G.; Lapkowski, M.; Quillard, S.; Pron, A.; Buisson, J. P.; Lefrant, S. *J. Phys. Chem.* **1996**, *100*, 6998.
(66) Cochet, M.; Louarn, G.; Quillard, S.; Buisson, J. P.; Lefrant, S. *J. Raman Spectrosc.* **2000**, *31*, 1041.
(67) Stammer, C.; Taurins, A. *Spectrochim. Acta* **1963**, *19*, 1625.
(68) Abasbegovic, N.; Vukotic, N.; Colombo, L. *J. Chem. Phys.* **1964**, *41*, 2575.
(69) Durnick, T. J. *J. Mol. Spectrosc.* **1971**, *39*, 536.
(70) Bandyopadhyay, I.; Manogaran, S. *J. Mol. Struct. (THEOCHEM)* **2000**, *507*, 217.
(71) Durnick, T. J.; Wait, S. C. *J. Mol. Spectrosc.* **1972**, *42*, 211.
(72) Biswas, N.; Umapathy, S. *J. Phys. Chem. A* **1997**, *101*, 5555.
(73) Francis, J. T.; Hitchcock, A. P. *J. Phys. Chem.* **1992**, *96*, 6598.
(74) Pavlychev, A. A.; Hallmeier, K. H.; Hennig, C.; Hennig, L.; Szargan, R. *Chem. Phys.* **1995**, *201*, 547.
(75) Hennig, C.; Hallmeier, K. H.; Bach, A.; Bender, S.; Franke, R.; Hormes, J.; Szargan, R. *Spectrochim. Acta A* **1996**, *52*, 1079.
(76) Hennig, C.; Hallmeier, K. H.; Szargan, R. *Synth. Met.* **1998**, *92*, 161.
(77) Nakajima, T.; Harada, M.; Osawa, R.; Kawagoe, T.; Furukawa, Y.; Harada, I. *Macromolecules* **1989**, *22*, 2644.
(78) Tan, K. L.; Tan, B. T. G.; Kang, E. T.; Neoh, K. G. *Phys. Rev. B* **1989**, *39*, 8070.
(79) Monkman, A. P.; Stevens, G. C.; Bloor, D. *J. Phys. D: Appl. Phys.* **1991**, *24*, 738.
(80) Zeng, X.-R.; Ko, T.-M. *Polymer* **1998**, *39*, 1187.

MA049054+